http://dx.doi.org/10.5012/bkcs.2014.35.1.182

Synthesis, Structures and Properties of Three Metal-organic Frameworks Based on 3-(4-((1*H*-imidazol-1-yl)methyl)phenyl)acrylic Acid

Peng Liang, Tian-Tian Ren, Wei-Man Tian, Wen-Jia Xu, Gang-Hong Pan, and Xian-Hong Yin*

College of Chemistry and Chemical Engineering, Guangxi University for Nationalities, Nanning 530006, P.R. China
**E-mail: 6628yxh@163.com*
Received August 21, 2013, Accepted October 23, 2013

Three new transition metal complexes based on Ozagrel $[Cu(Ozagrel)]_n$ (**1**), $[Zn(Ozagrel)(Cl)]_n$ (**2**), $\{[Mn_2(Ozagrel)(1,4\text{-ndc})_2]\cdot(H_2O)\}_n$ (**3**), (Ozagrel = 3-(4-((1H-imidazol-1-yl)methyl)phenyl)acrylic acid; 1,4-ndc = 1,4-Naphthalenedicarboxylic acid) have been hydrothermally synthesized and characterized by elemental analyse, IR, TG, PXRD, electrochemical analysis and single crystal X-ray diffraction. X-ray structure analysis reveals that **1** and **3** are 3D coordination polymers, while complex **2** is a two-dimensional network polymer, the 2D layers are further packed into 3D supramolecular architectures that are connected through hydrogen bonds. The electrochemistry of **1-3** was studied by cyclic voltammetry in methanol and water using a glassy carbon working electrode. Also, thermal decomposition process and powder X-ray diffraction of complexes were investigated.

Key Words : Crystal structures, 3-(4-((1*H*-imidazol-1-yl)methyl)phenyl)acrylic acid, Electrochemical analysis, Supramolecular architecture

Introduction

In last decades, the chemists have devoted themselves to the development of new crystalline materials with a variety of properties, functions, and potential applications such as gas sorption, luminescence, molecular magnetism, nonlinear optics, catalysis, and ion-exchange.[1-6] It is a very difficult task to design and predict a new metalorganic framework (MOF) structure with a specific net topology from the metal ion and organic linker used as the reactants. The same reactants can result in completely different framework structures, depending on the reaction conditions used, such as solvent, temperature, concentration and ratio of reactants, reaction time, and pH.[7-10]

To the best of our knowledge, selecting appropriate ligands is the most effective strategy in obtaining coordination polymers. The new network structures utilizing both covalent and hydrogen bonds have attracted much interests recently due to their flexible structural features.[11-13] Ozagrel is a novel anti-platelet aggregation agent, for the treatment of acute cerebral infarction and cerebral infarction associated with movement disorders in our daily life, and it consists of a imidazole ring, phenyl acrylate and they are connected together *via* a methylene group. Ozagrel (3-(4-((1*H*-imidazol-1-yl)methyl)phenyl)acrylic acid) is good candidates for the construction of novel metal–organic complexes, which show many important advantages than other organic ligands: (1) It has a carboxyl group that can completely or partially deprotonate, which provids rich coordination modes; (2) It contains an imidazole ring, and it can completely or partially deprotonate also; (3) It has unsaturated bond (C=C). It displays strong reactivity with metal ions, but rarely coordination polymers has been synthesized from the Ozagrel ligand, complexes constructed from Ozagrel are still largely unexplored.[14-16]

In this paper, we describe the syntheses of three novel complexes $[Cu(Ozagrel)]_n$ (**1**), $[Zn(Ozagrel)(Cl)]_n$ (**2**), $\{[Mn_2(Ozagrel)(1,4\text{-ndc})_2]\cdot(H_2O)\}_n$ (**3**), and we report crystal structures, elemental analyses, electrochemical analysis, IR spectroscopy and thermal properties of three novel complexes with Ozagrel ligands.

Experimental

All chemicals were commercial materials of analytical grade and used without purification. Elemental analysis for C, H, and N was carried out on a Perkin-Elmer 2400 II elemental analyzer. The FT-IR spectrum was obtained on a PE Spectrum One FT-IR Spectrometer Fourier transform infrared spectroscopy in the 4000-400 cm^{-1} regions, using KBr pellets. Powder X-ray diffraction patterns were obtained using a pinhole camera (Anton Paar) operating with a point focused Ni-filtered Mo-$K\alpha$ radiation in the 2θ range from 5° to 50° with a scan rate of 0.08° per second. Thermogravimetry analyzer was performed on Perkin-Elmer TG/DTA 6300 thermal analyzer under owing N_2 atmosphere at a heating rate of 10 $^oC\cdot min^{-1}$. Cyclic voltammetry were performed on a CHI 660C electrochemical workstation.

Synthesis of the Complex $[Cu(Ozagrel)]_n$ (1): To a stirred solution of Ozagrel (0.2274 g, 1 mmol) in 2 mL acetonitrile, 10 mL water and 8 mL ethanol was added dropwise with stirring at room temperature to a solution of $Cu(CH_3COO)_2\cdot H_2O$ (0.1996 g, 1 mmol) in the mixture of 5 mL water. Then an aqueous solution of sodium hydroxide was added dropwise with stirring to adjust the pH value of the solution being 6.5. The resulting mixture was sealed in a 30 mL Teflon-lined

stainless reactor, kept under autogenous pressure at 408 K for 72 h, and then slowly cooled to room temperature at a rate of 10 °C per hour. The blue block crystals suitable for X-ray diffraction were isolated directly, washed with ethanol and dried in air (0.196 g, Yield: 46%, based on Cu). Anal. Calcd for $C_{13}H_{11}CuN_2O_2$ (%): C, 53.70; H, 3.81; N, 9.63; Found: C, 53.48; H, 3.92; N, 9.86. IR data (KBr pellets, cm^{-1}): 1583 (m), 1566 (w), 1527 (m), 1423 (m), 1377 (vs), 1240 (vs), 1107 (w), 947 (m), 852 (w).

Synthesis of the Complex [Zn(Ozagrel)(Cl)]$_n$ (2): The same synthetic procedure as that for **1** was used except that Ozagrel (0.2296 g, 1 mmol), and $Cu(CH_3COO)_2·H_2O$ (0.1996 g, 1 mmol) was replaced by $ZnCl_2$ (0.1363 g, 1 mmol). The colorless crystals suitable for X-ray diffraction were isolated directly, washed with ethanol and dried in air (0.208 g, Yield: 57%, based on Zn). Anal. Calcd for $C_{13}H_{11}ZnN_2O_2Cl$ (%): C, 47.59; H, 3.38; N, 8.54; Found: C, 47.32; H, 3.47; N, 8.68. IR data (KBr pellets, cm^{-1}): 1642(vs), 1524 (vs), 1433 (w), 1234 (s), 1155 (m), 1091 (vs), 865 (m), 748 (vs).

Synthesis of the Complex {[Mn$_2$(Ozagrel)(1,4-ndc)$_2$]·(H$_2$O)}$_n$ (3): To a stirred solution of Ozagrel (0.1148 g, 0.5 mmol), 1,4-ndc (0.2162 g, 1 mmol) in 2 mL acetonitrile, 10 mL water and 8 mL ethanol was added dropwise with stirring at room temperature to a solution of $MnCl_2·4H_2O$ (0.1979 g, 1 mmol) in the mixture of 5 mL water. Then an aqueous solution of sodium hydroxide was added dropwise with stirring to adjust the pH value of the solution being 6. The resulting mixture was sealed in a 30 mL Teflon-lined stainless reactor, kept under autogenous pressure at 408 K for 72 h, and then slowly cooled to room temperature at a rate of 10 °C per hour. The colorless block crystals suitable for X-ray diffraction were isolated directly, washed with ethanol and dried in air (0.227 g, Yield: 43%, based on Mn). Anal. Calcd for $C_{37}H_{26}Mn_2N_2O_{11}$ (%): C, 56.65; H, 3.34; N, 3.57; Found: C, 56.37.48; H, 3.52; N, 3.83. IR data (KBr pellets, cm^{-1}): 3445 (w), 3144 (m), 1618 (m), 1564 (vs), 1508 (s), 1408 (vs), 1365 (vs), 783 (m), 567 (s).

Crystal Structure Determination. Diffraction experiments for **1**-**3** were carried out with Mo-*K*α radiation using a BRUKER SMART APEX CCD diffractometer at 296 K. The structures were solved by direct methods and refined with full-matrix least-squares on F^2 using SHELXS-97 and SHELXL-97.[17] All non-hydrogen atoms were refined aniso-

Table 1. Crystal data and structure refinements for **1**-**3**

Complex	**1**	**2**	**3**
Empirical formula	$C_{13}H_{11}CuN_2O_2$	$C_{13}H_{11}ZnN_2O_2Cl$	$C_{37}H_{26}Mn_2N_2O_{11}$
Formula weight	290.78	328.06	784.48
Temperature(K)	296(2)	296(2)	296(2)
Wavelength (Å)	0.71073	0.71073	0.71073
Crystal system	Monoclinic	Monoclinic	Monoclinic
Unit cell dimensions (Å)			
a	9.799(4)	12.534(2)	11.240(2)
b	9.799(4)	13.024(2)	12.641(2)
c	10.49(6)	9.3175(2)	11.628(2)
Volume (Å^3), Z	872.7(7), 3	1504.9(4), 4	1650.4(4), 2
Calculated density ($g·cm^{-3}$)	1.660	1.448	1.579
Absorption coefficient (mm^{-1})	1.870	1.807	0.834
F(000)	444	664	800
θ range for data collection (°)	2.40-24.95	2.27-25.00	1.75-25.00
Data/restraints/ parameters	2011/1/163	2580/366/173	4971/1/469
Goodness-of-fit on F^2	1.078	1.055	1.041
Final Ra indices [I>2σ(I)]	R1 = 0.0432 *w*R2= 0.1149	R1 = 0.0327 *w*R2 = 0.1041	R1 = 0.0473 *w*R2 = 0.1197
R indices (all data)	R1 = 0.0441 *w*R2= 0.1155	R1 = 0.0356 *w*R2= 0.1065	R1 = 0.0505 *w*R2 = 0.1277

Table 2. Selected bond lengths (Å) and angles (°) for **1**-**3**

	Complex **1**		
Cu(1)-N(1)#2	1.961(5)	Cu(1)-C(11)	2.044(5)
Cu(1)-O(1)#1	2.002(4)	Cu(1)-C(12)	2.006(6)
Cu(1)-O(2)#1	2.645(4)		
N(1)#2-Cu(1)-O(1)#1	104.3(2)	N(1)#2-Cu(1)-C(11)	111.2(2)
N(1)#2-Cu(1)-C(12)	151.0(2)	O(1)#1-Cu(1)-C(11)	143.8(2)
O(1)#1-Cu(1)-C(12)	104.4(2)	C(12)-Cu(1)-C(11)	39.9(2)
O(2)#1-Cu(1)-N(1)#2	96.81(2)	O(2)#1-Cu(1)-O(1)	54.96(2)
O(2)#1-Cu(1)-C(11)	124.7(2)	O(2)#1-Cu(1)-C(12)	102.5(2)
	Complex **2**		
Zn(1)-O(1)#3	1.980(2)	Zn(1)-N(1)	2.000(2)
Zn(1)-O(2)#4	1.995(2)	Zn(1)-Cl(1)	2.211(8)
O(1)#3-Zn(1)-O(2)	101.8(8)	O(1)-Zn(1)-Cl(1)	116.8(7)
O(1)#3-Zn(1)-N(1)	110.4(9)	O(2) -Zn(1)-Cl(1)	107.0(6)
O(2)#4-Zn(1)-N(1)	102.2(9)	N(1)-Zn(1)-Cl(1)	116.4(6)
	Complex **3**		
Mn(1)-O(8)	2.114(4)	Mn(1)-O(6)#5	2.130(4)
Mn(1)-O(9)#6	2.149(4)	Mn(1)-O(4)#7	2.152(4)
Mn(1)-O(2)	2.294(3)	Mn(1)-O(1)	2.327(3)
Mn(2)-O(7)	2.122(3)	Mn(2)-O(10)#8	2.136(3)
Mn(2)-O(5)#5	2.172(3)	Mn(2)-O(2)	2.209(4)
O(8)-Mn(1)-O(6)#5	98.91(2)	O(8)-Mn(1)-O(9)#6	83.90(2)
O(6)#5-Mn(1)-O(9)	106.8(4)	O(8)-Mn(1)-O(4)#7	164.8(2)
O(6)-Mn(1)-O(4)#7	92.75(2)	O(9)-Mn(1)-O(4)#7	83.55(2)
O(8)-Mn(1)-O(2)	91.52(4)	O(6)#5-Mn(1)-O(2)	86.99(3)
O(9)#6-Mn(1)-O(2)	165.9(4)	O(9)#6-Mn(1)-O(2)	165.9(4)
O(4)#7-Mn(1)-O(2)	98.69(3)	O(8)-Mn(1)-O(1)	93.19(3)
O(6)#5-Mn(1)-O(1)	141.9(3)	O(9)#6-Mn(1)-O(1)	110.3(4)
O(4)#7-Mn(1)-O(1)	83.33(4)	O(2)-Mn(1)-O(1)	56.57(2)
O(7)-Mn(2)-O(10)	164.9(2)	O(7)-Mn(2)-O(5)#5	99.96(2)
O(10)-Mn(2)-O(5)	90.75(3)	O(7)-Mn(2)-O(2)	96.43(2)
O(10) -Mn(2)-O(2)	95.99(4)	O(5)#5-Mn(2)-O(2)	79.27(2)
O(7)-Mn(2)-O(3)	84.23(4)	O(10)-Mn(2)-O(3)	86.93(3)
O(5)#5-Mn(2)-O(3)	170.1(2)	O(2)-Mn(2)-O(3)	91.42(4)
O(7)-Mn(2)-O(1)#9	85.40(2)	O(10)-Mn(2)-O(1)	86.00(4)
O(5)-Mn(2)-O(1)#9	80.14(2)	O(2)-Mn(2)-O(1)#9	159.3(3)

Symmetry transformations used to generate equivalent atoms: #1 −x+y, −x, z+1/3; #2 −y, x−y, z−1/3; #3 −x+1, y+1/2, −z+1/2; #4 −x+1, −y+2, −z; #5 x, y, z−1; #6 −x+2, y+1/2, −z+1; #7 −x+1, y+1/2, −z+1; #8 x−1, y, z; #9 −x+1, y−1/2, −z+1

tropically. Hydrogen atoms were placed at geometrically calculated positions by using a riding model. A summary of the crystallographic data and structure refinements was shown in Table 1, selected bond lengths and angles of the complexes were listed in Table 2, and hydrogen bond geometries were given in Table 3.

Crystallographic data for the structures reported here have been deposited with CCDC (Deposition No. CCDC-953511 (**1**), No. CCDC-953513 (**2**), No. CCDC-953512 (**3**)). These data can be obtained free of charge *via* http://www.ccdc.cam.ac.uk/conts/retrieving.html or from CCDC, 12 Union Road, Cambridge CB2 1EZ, UK, E-mail: deposit@ccdc.cam.ac.uk.

Results and Discussion

Description of the Structure. The single-crystal X-ray diffraction analysis reveals that the complex **1** is crystallize in the trigonal system with space group *P*3(2), while complex **2** and **3** are both crystallize in the monoclinic system with space group *P*2(1)/*c* and *P*2(1).

ORTEP-3 view of the molecular structure of **1** is depicted in Figure 2(a), The selected molecular geometry parameters are listed in Table 2. The X-ray crystal analysi of complex **1** revealed that one Cu(I) ion and a completely deprotonated Ozagrel anion. The coordination environment around the Cu(I) center is best portrayed as a distorted tetrahedron geometry, ligated by two oxygen atoms (O1#1, O2#1), one nitrogen atom from a Ozagrel anion (N1#2) and non benzene ring double bond from another Ozagrel molecule (Figure 2(b)). The Zn–O bond lengths vary from 2.002(4) to 2.645(4) Å, the Zn–N bond lengths is 1.961(5) Å, while the Zn-N bond length short than the Zn–O bond. Furthermore, the distances of Cu–C11 and Cu–C12 are 2.044(5) and 2.006(6) Å, respectively, and the distance from Cu(I) to the double bond is 1.903(3) Å. The C=C bond distance (1.382(8) Å) of the coordinated olefin is longer than that in free ozagrel (1.324(5) Å). The lengthening of the C=C distance is typical for ethylene that is η^2-bonded to low-valent, electron-rich, transition metals such as copper(I). The coordination mode of $[Ozagrel]^{2-}$ in this complex is shown in Figure 1a. Ozagrel anion acting as a tridentate linker is coordinated to

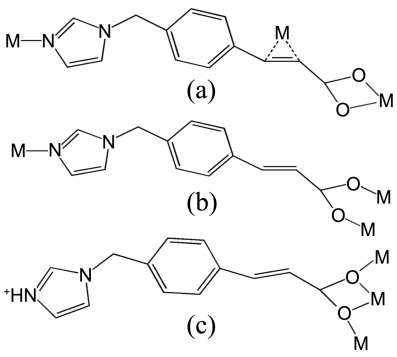

Figure 1. (a) Coordination modes of Ozagrel in complex **1**; (b) Coordination modes of Ozagrel in complex **2**; (c) Coordination modes of Ozagrel in complex **3**.

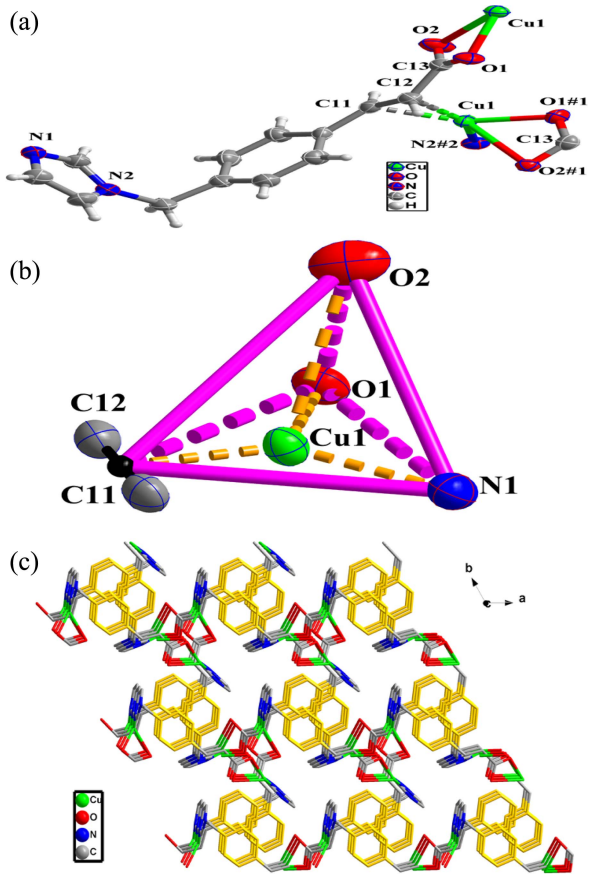

Figure 2. (a) The coordination environment of Cu(I) ion of the complex **1**; (b) The coordination polyhedra of **1**; (c) The 3D supramolecular architecture of **1** along c-axis (H atoms are omitted for clarity).

Cu(I) ion generating a three dimensional coordination polymer based on one-dimensional helical chain of Cu(I) centers. If the node is copper, three ligands attached to it as a "fan-like" and extending outwardly, since the bending angle of the ligand itself, it form 3D supramolecular architectures final (Figure 2(c)). In other words, 3(2)-pyridylacrylic acid resulted in two-dimensional coordination layers by metal coordination to Cu(I) ion while more flexible ozagrel gave rise to a three-dimensional coordination framework. The flexible molecular structure of ozagrel could play the subtle role in the final extended structure.

The molecular structure of complex **2** with the atom numbering scheme is shown in Figure 3(a), In the structure, each Zn(II) center is four-coordinated by two carboxylate sp^3 oxygen atoms (O1#1, O2#2) from other two deprotonated [Ozagrel] ligands, one imidazole nitrogen atom (N1) from another deprotonated [Ozagrel] ligand and one chloride ions (Cl1). The Zn–O bond lengths are 1.9806(17) Å [Zn–O1#1] and 1.9954(19) Å [Zn–O2#2], and they are slightly shorter than the length of 2.000(2) Å [Zn–N1] and 2.2109(8) Å [Zn–Cl1] (Table 2), which both are within the normal ranges. The coordination mode of $[Ozagrel]^{2-}$ in this complex is shown in Figure 1(b), a ligand also connect with three Zn(II) metal centers, but it is different from **1**. Because the ligand itself is

Table 3. Hydrogen-bond geometry (Å) and angles (°) for complexes

D-H···A	D-H	H···A	D···A	D-H···A
Complex **2**				
C(10)-H(10B)···Cl(1)	0.969	2.790	3.742(4)	167.37
C(13)-H(13)···Cl(1)	0.929	2.749	3.629(4)	158.32
Complex **3**				
O11–H(11B)···O(6)	0.85	2.09	2.879(7)	154.0
N1–H(1)···O(3)	0.86	2.06	2.890(6)	163.5

bent, the two planes based on benzene and imidazole in a Ozagrel intersect at right angles, so two ligands and two Zn(II) centers connected together to form a quadrilateral by N1, O2, than the two quadrilaterals connected together by O1, thus giving rise to the formation of a 2D layer framework (Figure 4), However, unlike most of the 2D grid networks, it is not co-planar but double undulated, resulting from the inherent bent conformations of the Ozagrel molecules. In **2**, chloride ions are used to balance the charge, there is no direct role of bridge. In addition, it can be seen that there exist two kinds of intermolecular hydrogen bonds in the crystal structure. The uncoordinated oxygen atom of [Ozagrel] in **2** forms two intermolecular weak C-H···Cl hydrogen bonds [C(10)-H(10B)···Cl(1) 3.742(4) Å, C(13)-H(13)···Cl(1) 3.629(4) Å] with the hydrogen on the carbon atom of imidazole ring from the ligand, and -CH_2- hydrogen in the ligand, respectively. The coordinated chloride atom of the ligand connects the two neighboring 2D structures through the other axis to form a 3D supramolecular structure. The above-mentioned hydrogen bonds also play a key role in stabilizing the 3D supramolecular structure (Figure 3(b)).

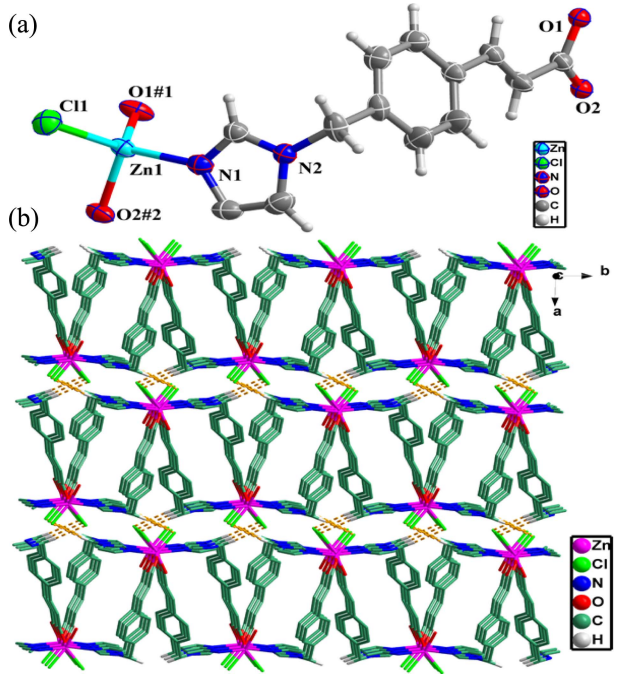

Figure 3. (a) The coordination environment of Zn(II) ion of the complex **2**; (b) The 3D supramolecular architecture of **2** with hydrogen bonds. The hydrogen bonds are indicated by dashed lines.

Single crystal X-ray diffraction analysis shows that the asymmetric unit of **3** consists of two of Mn(II) ions, one deprotonated Ozagrel, two completely deprotonated [1,4-ndc]$^{2-}$ anions and a free water. As depicted in Figure 5(a), The Mn1 cation is surrounded by six oxygen atoms, four belong to monodentately (Mn–O: 2.152 Å, 2.130 Å, 2.114 Å, 2.149 Å), and two to bidentately chelating coordinating carboxylate groups (Mn–O: 2.327 Å, 2.294 Å), the Mn–O bonds lengths vary from 2.114 to 2.327 Å. The Mn2 cation is also surrounded by six oxygen atoms, but all of the atoms belong to monodentately (Mn–O: 2.122 Å, 2.136 Å, 2.172 Å, 2.209 Å, 2.215 Å, 2.232 Å) from two Ozagrel ligands and four 1,4-ndc ligands, the Mn–O bonds lengths vary from 2.122 to 2.232 Å. Coordination mode of [Ozagrel]$^{2-}$ in **3** is shown in Figure 1(c), a Ozagrel connect with three Mn(II)

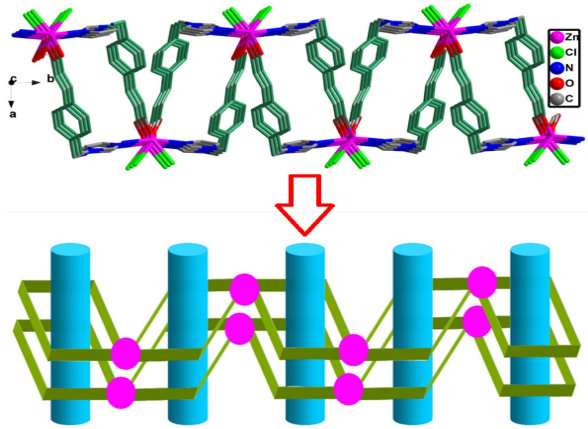

Figure 4. The 2D layered network of complex **2**. Unnecessary atoms are omitted for clarity.

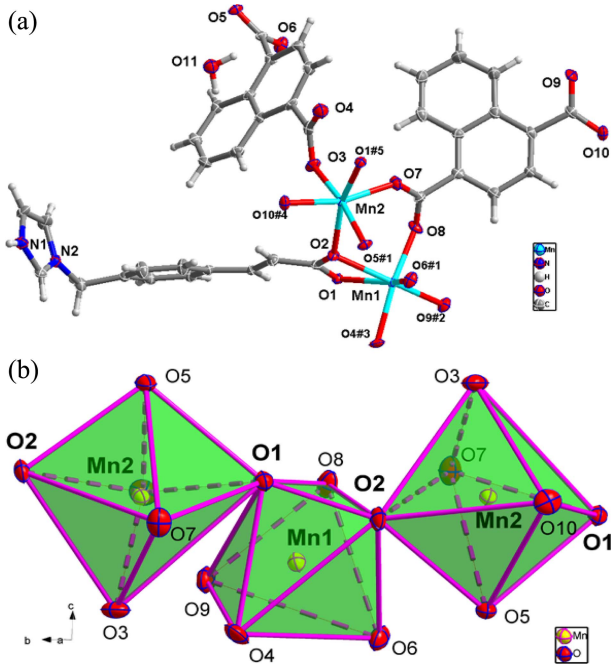

Figure 5. (a) The coordination environment of Mn(II) ion of the complex **3**; (b) The coordination polyhedra of **3**.

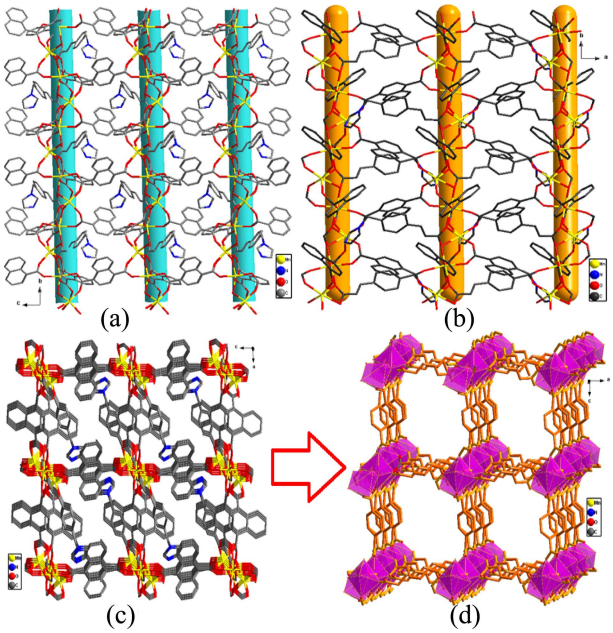

Figure 6. (a) The 3D supramolecular architecture of **3** along a-axis; (c) The 3D supramolecular architecture of **3** along c-axism; (b) and (d) The 3D supramolecular architecture of **3** along b-axis.

metal centers (μ_3-η^4), a 1,4-ndc connect with four Mn(II) metal centers (μ_4-η^4). In Ozagrel, two crystallographically independent Mn(II) metal centers can be connected to a metal chain in the role of the carbonyl oxygen. Both MnO_6 octahedra are bridged by carboxylate groups to form a dimer (Mn1–Mn2 = 3.528 Å, Mn1–Mn2' = 3.738 Å). More details of the coordination modes of the bridging carboxylates are given in ref 18. The metal chains form 1D tunnel in the bridging role of the $[ndc]^{2-}$, finally, we obtain 3D supramolecular pore structure, free water molecules and Ozagrel are filled in these holes (Figure 5(b), Figure 6).

IR Spectra. The IR spectra of free ligand (Ozagrel) shows strong bands of the carboxylate groups at 1676 cm^{-1}, which can be assigned as the μ(C=O) antisymmetric stretching vibrations. In addition, The COO is coordinated with its asymmetric and symmetric stretching appearing at 1566 and 1377 cm^{-1} in **1**, 1524 and 1433 cm^{-1} in **2**, 1564 and 1365 cm^{-1} in **3**, beacuse the shift suggests that the relevant oxygen of the ligand coordinates to metal. In complex **1**, there are no absorption bands at about 1700-1600 cm^{-1}, and description carbonyl and C=C double bond are involved in the reaction. ν_sC=C appears medium intensity peaks at 1642 cm^{-1} in **2**. In the IR spectra of complex **3**, the strong and broad absorption bands at about 3445 cm^{-1} are attributed to the symmetric O–H stretching modes, and the N–H stretching band at 3144 cm^{-1}.

XRD Patterns. In order to confirm the phase purity of these polymers, the X-ray powder diffraction patterns of polymer **2** and **3** are measured and shown in Figure 7. It is clearly seen that the peak positions in the experimental PXRD patterns are in good agreement with the correspondingly simulated ones except the differences in intensity, which indicate a pure phase of each bulk sample. The difference in

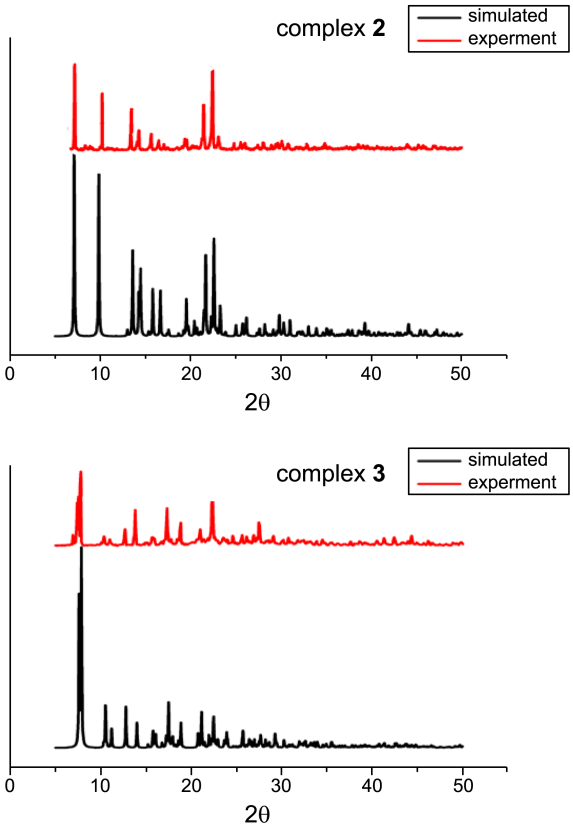

Figure 7. Simulated and experimental PXRD spectra of polymers **2** and **3**.

reflection intensity between the simulated and experimental patterns is due to preferred orientation of the powder samples during data collection.

Electrochemical Studies. The cyclic voltammetric measurement of **1-3** (1 $mmol \cdot L^{-1}$) have been recorded at 25 °C in methanol and water solutions containing 0.05 $mol \cdot L^{-1}$ $LiClO_4$ (pH=10.78) supporting electrolyte at a glassy carbon working electrode at scan rates of 100 mV s^{-1}. The complex **1** displays one couple of oxidation/reduction peaks (Figure 8(a)), which corresponds to Cu(II)/Cu(I) and Cu(I)/Cu(0).[19] The mean peak potential $E_{1/2}$ = (Epa+Epc)/2 was 0.096 V and –0.511 V, respectively. **2** displays one couple of oxidation/reduction peaks (Figure 8(b)), which corresponds to Zn(II)/Zn(0). Electric potentials of cathode and anode are Epc = –1.317 V and Epa = –1.136 V with $E_{1/2}$ = –1.226 V. From ΔE (0.181 V) and I_{pa}/I_{pc} (–0.15), the electron transfer is quasi-reversible. While for **3**, Since the ligands show no electrochemical response up to –0.7 V, a quasi-reversible redox peak attributed to redox of Mn(II)/Mn(0) was observed. The mean peak potential $E_{1/2}$ = (Epa+Epc)/2 was –0.151 V for **3** (Figure 8(c)).

Thermogravimetric (TG) Analyses. In order to examine the thermal stabilities of the complexes, thermal gravimetric (TG) were carried out by heating **1-3** in nitrogen at the heating rate of 10 $^oC \cdot min^{-1}$, and the TG curves are shown in Figure 9. The TG indicates that the complex **1** is display mainly one step of weight loss. The weight loss of 75.4% between 402 °C and 543 °C corresponds to the loss of Ozagrel

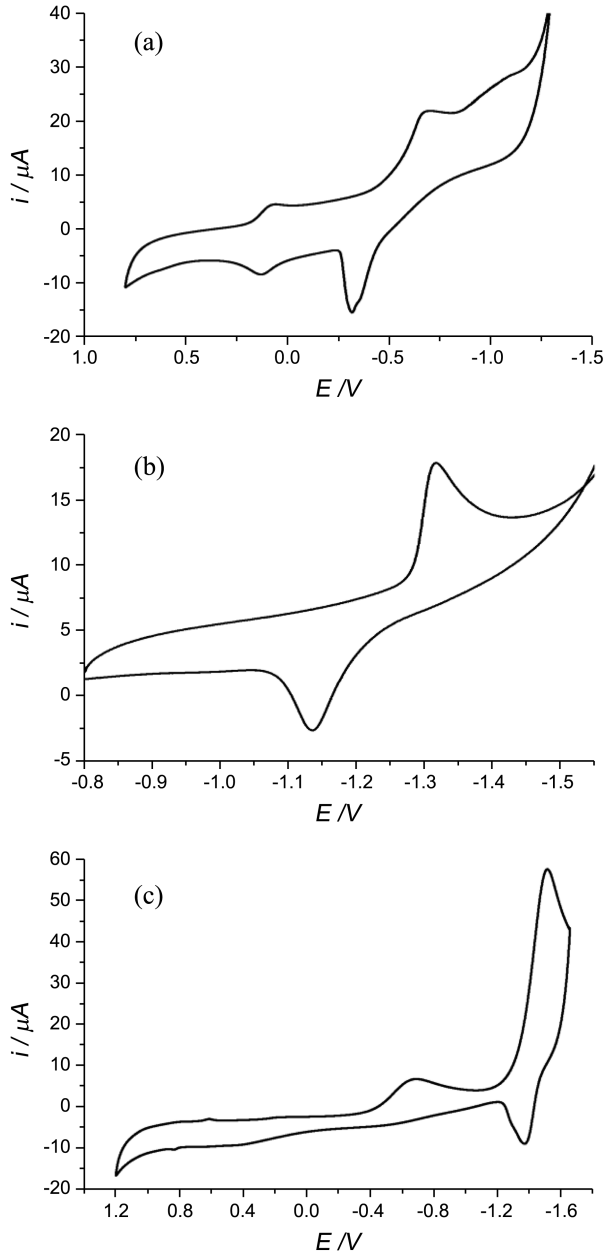

Figure 8. Cyclic voltammograms of complexes **1**-**3** measured at room temperature.

(Calc. 77.8%). The thermal behaviors of complex **2** are display mainly two steps of weight losses. The first step with 65.7% weight-loss from 348 to 496 °C corresponds to the release of coordination Ozagrel molecules (calculated: 68.8%) then it stable up to 542 °C. The second with weight loss of 11.4% between 542 and 567 °C corresponds to the two H_2dpa (calc. 10.8%). The final residue 22.9% could be corresponded to ZnO (calculated: 24.6%). In **3**, there are main three stages, the first starts from 78 to 146 °C with a mass loss of 3.1%, corresponding to loss of the water molecules (theoretical loss 2.3%), then it stable up to 283 °C. The second stage occurs in the 283-395 °C range with mass loss of 52.6% (calculated 54.7%) that correlate with elimination of 1,4-ndc molecules. The third stage in the 496-574 °C

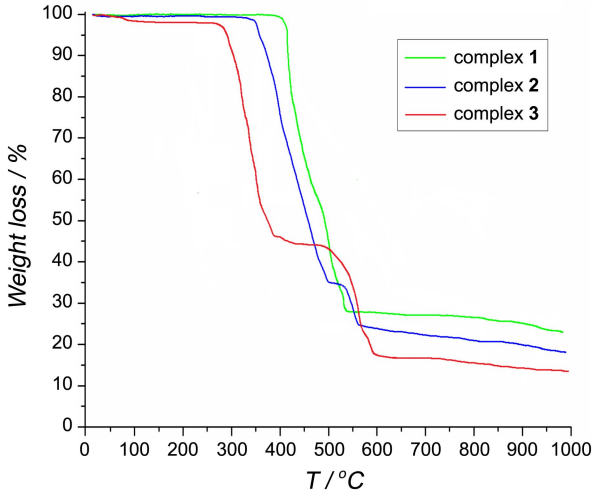

Figure 9. The TG curves of three complexes.

range corresponding to release of Ozagrel molecules with weight losses of 26.1% (calculated 28.7%). The final residue 19.1% could be corresponded to MnO (calculated: 18.1%).

Conclusion

In this work, we reported the synthesis and characterization of complexes $[Cu(Ozagrel)]_n$ (**1**), $[Zn(Ozagrel)(Cl)]_n$ (**2**), $\{[Mn_2(Ozagrel)(1,4\text{-ndc})_2]\cdot(H_2O)\}_n$ (**3**) by spectral method (IR), elemental analysis, thermal analysis, PXRD, electrochemical analysis and single-crystal X-ray diffraction techniques. The above results show that the configuration of Ozagrel plays an important role in affecting the final structure of the coordination polymers. The complexes of **1** and **3** are all 3D structure, and the complex **2** through hydrogen bonds hydrogen bonds interlink form the 2D layers to generate 3D supramolecular architectures. These complexes have different coordination modes, this means that Ozagrel will be many deep development. The complexes exhibit ligand-based good electrochemical properties, and good thermal stability with a decomposition temperature up to 300 °C.

Acknowledgments. This work was financially supported by the Innovation Project of Guangxi University for Nationalities (gxun-chx2012090), P. R. China. And the publication cost of this paper was supported by the Korean Chemical Society.

References

1. Zhang, Y. B.; Zhang, W. X.; Feng, F. Y.; Zhang, J. P.; Chen, X. M. *Angew. Chem. Int. Ed*. **2009**, *48*, 5287.
2. Williams, N. J.; Gan, W.; Reibenspies, J. H.; Hancock, R. D. *Inorg. Chem*. **2009**, *48*, 1407.
3. Song, Y.; Ohkoshi, S.; Arimoto, Y.; Seino, H.; Mizobe, Y.; Hashimoto, K. *Inorg. Chem*. **2003**, *42*, 1848.
4. Kumar, A.; Mayer-Figge, H.; Sheldrick, W. S.; Singh, N. *Eur. J. Inorg. Chem*. **2009**, *18*, 2720.
5. Farrusseng, D.; Aguado, S.; Pinel, C. *Angew. Chem. Int. Ed*. **2009**, *48*, 7502.
6. Zheng, S. L.; Zhang, J. P.; Wong, W. T.; Chen, X. M. *J. Am. Chem.*

Soc. **2003**, *125*, 6882.
7. Yaghi, O. M.; O'Keeffe, M.; Ockwig, N. W.; Chae, H. K.; Eddaoudi, M.; Kim, J. *Nature* **2003**, *423*, 705.
8. Wang, X. S.; Ma, S.; Yuan, D.; Yoon, J. W.; Hwang, Y. K.; Chang, J. S.; Wang, X.; Jørgensen, M. R.; Chen, Y. S.; Zhou, H. C. *Inorg. Chem*. **2009**, *48*, 7519.
9. Blake, A. J.; Champness, N. R.; Hubberstey, P.; Li, W. S.; Withersby, M. A.; Schroder, M. *Coord. Chem. Rev.* **1999**, *183*, 117.
10. Fomulu, S. L.; Hendi, M. S.; Davis, R. E.; Wheeler, K. A. *Cryst. Growth Des*. **2002**, *2*, 637.
11. Evans, R. C.; Douglas, P.; Winscom, C. J. *Coord. Chem. Rev.* **2006**, *250*, 2093.
12. Yong, B. G.; Wang, X. Q.; Ekaterina, V. A.; Allan, J. J. *Inorg. Chem.* **2005**, *44*, 8265.
13. Sun, F.; Koh, K.; Ryu, S. C.; Han, D. W.; Lee, J. *Bull. Korean Chem. Soc*. **2012**, *33*, 3950.
14. Lee, W. Z.; Kang, Y. L.; Wang, T. L.; Su, C. C.; Kuom, T. S. *Cryst. Growth Des*. **2008**, *8*, 2614.
15. Zhang, M.; Wang, R. R.; Chen, M.; Zhang, H. Q.; Sun, S.; Zhang, L. Y. *Chin. J. Nat. Med*. **2009**, *7*, 105.
16. Pan, C. L.; Xu, J. Q.; Chu, D. Q.; Ye, L.; Lu, Z. L.; Wang, T. G. *Inorg. Chem. Commun*. **2003**, *6*, 233.
17. Sheldrick, G. M. SHELXTL V5.1 software reference manual. Bruker AXS, Inc, Madison, Wisconsin, USA, 1997.
18. Cheng, M. L.; Zhu, E.; Liu, Q.; Chen, S. C.; Chen, Q.; He, M. Y. *Inorg. Chem. Commun*. **2011**, *14*, 300.
19. Widmann, A.; Kahlert, H.; Petrovic-Prelevic, I.; Wulff, H.; Yakhmi, J. V.; Bagkar, N.; Scholz, F. *Inorg. Chem*. **2002**, *41*, 5706.